Temperature Distribution in Friction Stir Welding Using Finite Element Method

Armansyah, I. P. Almanar, M. Saiful Bahari Shaari, M. Shamil Jaffarullah, Nur'amirah Busu, M. Arif Fadzleen Zainal Abidin, M. Amlie A. Kasim

***Abstract*—**During welding, the amount of heat present in weld zones determines the quality of weldment produced. Thus, the heat distribution characteristics and its magnitude in weld zones with respect to process variables such as tool pin-shoulder rotational and traveling speed during welding is analyzed using thermal finite element analyses method. For this purpose, transient thermal finite element analyses are performed to model the temperatures distribution and its quantities in weld-zones with respect to process variables such as rotational speed and traveling speed during welding. Commercially available software Altair HyperWork is used to model three-dimensional tool pin-shoulder vs. workpieces and to simulate the friction stir process. The results show that increasing tool rotational speed, at a constant traveling speed, will increase the amount of heat generated in weld-zones. In contrary, increasing traveling speed, at constant tool pin-shoulder rotational speeds, will reduce the amount of heat generated in weld zones.

***Keywords*—**Frictions Stir Welding, Temperature Distribution, Finite Element Method, Altair Hyperwork.

I. Introduction

FRICTION Stir Welding (FSW) was invented and patented by The Welding Institute in the UK in 1991. Principally the FSW is a joining process that employs a cylindrical shouldered tool with a probe (pin), rotates and plunges into the two consecutive parts of workpieces, and furthermore traverses slowly along the joint line to produce weldment [1]-[3]. Heat generated by friction between rotated tools (shoulder and pin) and the workpieces, is subjected in such a way to soften material of workpieces so that easy to be welded. As an efficient and effective welding process known as an environmentally friendly technique due to using no filler material, FSW has been expanded to be used in a variety of applications such as automotive, aerospace, railway, ship building/marine, oil and gas, construction etc. [4], [5]. The demand in manufacture industries nowadays can be seen a push towards application of lightweight metals but strong enough like Aluminum [6]. The joint type of two consecutive workpieces in this study is butt joint which is referred also to the welding line [7]. During the process tools are subjected to two simultaneous motions i.e. rotational and translational motions. In rotational motion the tools rotate which referred to the selected rotational speed (RS) in revolutions per-minute (RPM). In translational motion, the rotated tools travels along the welding line with selected feed rates or travel speeds (TS) in millimeters per minute (mm/min) or millimeters per second (mm/s) [8]. The half sides of friction stir welded region located on the left side of welding direction is called the retreating side, and on the right side of welding direction is called advancing side [9].

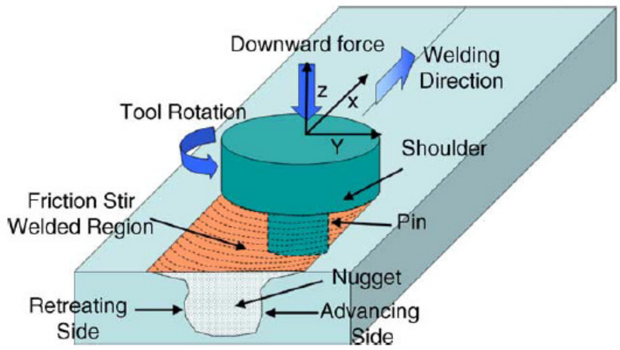

Fig. 1 Friction Stir Welding process schematic [2]

The forces act on the tools during the process are subjected in two dimensional axis X-Z which refer to as the longitudinal/travel force (F_x) according to the welding direction and axial force or downward force (F_z) respectively as shown in Fig. 1. This research focuses on a finite element analysis of friction stir process to facilitate better understanding of the fundamental knowledge of the process to find the optimum temperature in weld-zones which is required [10].

II. Heat Generation

The initial model of friction stir process approached the approximated estimation of the heat generation during welding. Gould and Feng developed a preliminary thermal model of FSW using the Rosenthal Equations to describe a moving heat source [11]. The heat input was described as a function of process parameters such as tool's rpm and tool's forces. Chao, Qi and Tang [12] formulated a boundary value problem for tool and workpiece [13]. They determined the frictional heat flux from the measured transient temperature fields obtained in the finite element analyses. In an attempt to predict the flow of material around the tool, Cole grove presented a finite element based thermal model of FSW [14].

A. Temperature Distribution

During the friction stir process, heat is generated through friction on the contact areas between tool and workpiece.

Armansyah, I.P. Almanar and M. Saiful Bahari Shaari are lecturer at Faculty of Mechanical Engineering, Universiti Teknologi MARA, Malaysia (e-mail: syah91@yahoo.com).

M. Shamil Jaffarullah, Nur'Amirah Busu, M. Arif Fadzleen Zainal Abidin, and M. Amlie M. Kasim are research assistants at the Faculty of Mechanical Engineering, Universiti Teknologi MARA, Malaysia.

World Academy of Science, Engineering and Technology
International Journal of Mechanical and Mechatronics Engineering
Vol:8, No:10, 2014

Those areas are on the shoulder butt surface, on the pin or probe side's surface, and on the pin tip surface (Q3) respectively. Friction on the shoulder butt surface occurs due to axial force from the rotated tool against workpiece surface in transverse plane. Contrastingly, friction on the pins side surface emerges as a result of travel force from the rotated tool against internal workpiece in coronal plane. On the pin tip surface, friction comes up from the rotating tool against internal workpiece in transvers plane. The tools are designed intentionally by using simple cylindrical flat shoulder surface and cylindrical flat pin surface. The simple model of tools is labeled with RS and RP that represents the radius of the shoulder and pin respectively, and HP represents as a height of pin. Fig. 2 shows the heat generations on the shoulder but surface (Q1), on the pin's side surface (Q2), and on the pin tip surface (Q3). The total heat generation can be represented as follows:

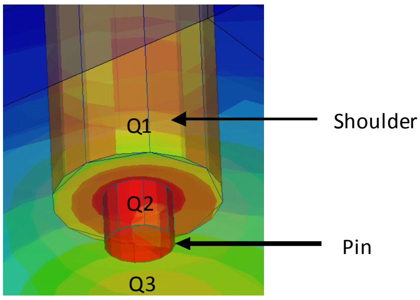

Fig. 2 Three-dimensional model of the friction stir welding process

The heat generated in each contact surface can then be computed as:

$$Q_{total} = Q_1 + Q_2 + Q_3 \tag{1}$$

$$dQ = \omega dM = \omega r dF = \omega r \tau_{contact} dA \tag{2}$$

where M is the moment, F is the force, A is the contact area and r is the cylindrical coordinate. According to the modified Coulomb's friction law,

$$\tau_{contact} = \mu P \tag{3}$$

while pressure P can be expressed in term of force, F and contact area, A:

$$P = \frac{F}{A} \tag{4}$$

Equations (1) to (4), the pressure has the relationship with the travel speed of the tool (TS) since the analysis of the heat generation was considered mainly during traveling. Pressure has the proportional relationship with the force, while force has the proportional relationship to power. The relationship of power with the travel speed (TS) or v_{tool} can be expressed as:

$$Power = F \times v_{tool} \tag{5}$$

In this study, it is considered to analyze temperatures on the contact area that undergoes friction significantly in an effort to generate heat to soften material of the workpiece. This occurs mainly in between the pin's side surface and internal workpiece. Thus a frictional area can be expressed to (6), where R_p and H_p are the radius and the height of the pin respectively:

$$A = \pi R_p H_p \tag{6}$$

Furthermore, the heat generation at the pin's side surface can be derived by integrated both side:

$$Q = \int_0^{2\pi} \int_0^{H_p} \omega r^2 \mu P \, dz \, d\theta \tag{7}$$

$$Q = 2\pi \, \omega \, \mu \, P \, R_p^2 H_p \tag{8}$$

Express angular rotational speed, ω in term of rotational speed, N in (rot/s) by substitute $\omega = 2\pi N$, heat generation equation at the probe's side surface:

$$Q = 4\pi^2 \, N \, \mu \, P \, R_p^2 H_p \tag{9}$$

Heat generation can be converted to temperature by considering the physical properties of the Aluminum Alloy 6061–T6 such as specific heat capacity and density of the material. Temperatures in weld zone are very important since it's necessary to soften material of the workpiece in conjunction to produce weldment. Therefore determining the suitable value of travel speed (TS) as well as rotational speed (RS) in relation to the required weld zone temperatures is necessary to carry out in order to improve the best quality of weldment. The relationship between temperature and heat generation can be expressed as follows:

$$Q = c_p \, \rho \, T \tag{10}$$

A. Heat Input

Theoretically heat input relies on rotational speed (RS) and travel speed (TS) which both are the main process variables in friction stir process. The initial temperature of the workpiece is assumed equal to the ambient temperature (25˚C). Convection's coefficient of 30 W/m˚C is applied at the top and side surfaces of the workpiece. Since the value of conductive coefficient between the workpiece and the backing plate is unknown, convective coefficient of 300 W/m˚C can be applied to the bottom surface of the work piece [15].

Investigation in the influence of the rotational speed on the spatial distribution, Tang reported temperature range between 425˚C and 475˚C once the rotational speed increased from 300 up to 1000 rpm for 6061-T6 by using a tool of 20 mm of shoulder's diameter and 6.5 mm of pin's diameter. Temperature drop was found between 340˚C and 375˚C within less than 10mm of the centerline [8].

Generally the significant temperatures of workpiece's material in weld zones during friction stir process in Aluminum based alloys can be reached around 400˚C - 650˚C whereby the material undergoes solid-state until melting. The highest temperature is observed in the area near to the pin side's surface, where the maximum heat flux exists. Temperature will continuously increase together with increasing the rotational speed (RS), decreasing the feed rate, or precisely the pseudo-heat index, and an increasing in the plunge depth [16]. Thermocouple can be concluded that the temperatures generated do not appear to be strongly influenced by the alloy type in most cases, except when the incipient melting temperature is exceeded, which is in any case undesirable for weld integrity [17]. Applying reliable thermocouple measurements within the welding process demands the need for computer simulation models to be expected to predict the temperatures distribution in the weld zones.

III. Material

Aluminum Alloy 6061-T6 is one of the most extensively used of the 6000 series Aluminum alloys. It is a versatile heat treatable extruded alloy with medium to high strength capabilities. Typical properties of Aluminum alloy 6061 include: medium to high strength, good toughness, good surface finish, excellent corrosion resistance to atmospheric conditions, good corrosion resistance to sea water, can be anodized, good weld ability and good workability and widely available. Alloy 6061 is typically used for heavy-duty structures in rail coaches, truck frames, shipbuilding, bridges and military bridges, aircraft and aerospace applications including helicopter rotor skins, tube, pylons and towers, transport, motorboats and rivets. The Element's components of AA6061–T6 that is used in this study can be seen in the Table I.

TABLE I
Element Component in 6061-T6 Aluminium Alloy

Symbol	Quantity
Al	95.8-98.6
Cr	0.04-0.35
Cu	0.15-0.4
Fe	Max 0.7
Mg	0.8-1.2
Mn	Max 0.15
Si	0.4-0.8
Ti	Max 0.15
Zn	Max 0.25
Al	95.8-98.6
Cr	0.04-0.35
Cu	0.15-0.4
Fe	Max 0.7
Other, each	Max 0.05
Other, total	Max 0.15

In order to calculate the heat generation produced during the temperature of 450˚C and 550˚C, the physical properties and thermal properties of this material need to be considered (see Table II). It is a cold welding process performed at a temperature lower than its melting point. It is similar to cold extrusion process. FSW is performed by plunging a rotating cylindrical tool, into the two adjustment workpieces and translating the tool along the direction of the intended weld with a controlled linear and angular velocity. The weldment is produced due to severe plastic deformation of the material around the rotating tool. FSW of Aluminum can be successfully performed by prescribing a welding speed of 1-10mm/s and rotational velocity in range of 400-1200 rpm [18].

TABLE II
6061-T6 Aluminium Properties

Physical Properties	**Metric**	**English**
Density	2.7g/cc	0.0975ib/in^3
Mechanical Properties		
Hardness, Rockwell B	60	60
Hardness, Vickers	107	107
Ultimate Tensile Strength	310MPa	45000psi
Tensile Yeild Strength	276MPa	40000psi
Elongation at Break	12%	12%
Modulus of Elasticity	68.9GPa	10000ksi
Poisson Strength	0.33	0.33
Fatigue Strength	96.5MPa	14000psi
Fracture Toughness	29MPa-m$_{1/2}$	26.4ksi-in$_{1/2}$
Shear Strength	207MPa	30000psi
Thermal Properties		
Thermal Conductivity	167W/m-K	1160BTU-in/hr-ft^2-°F
Melting Point	583-652°C	1080-1205°F

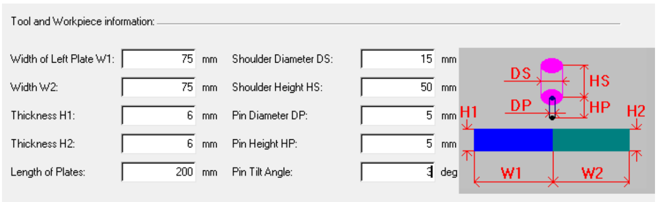

Fig. 3 Modeling tool and workpieces of FSW by HyperXtrude software

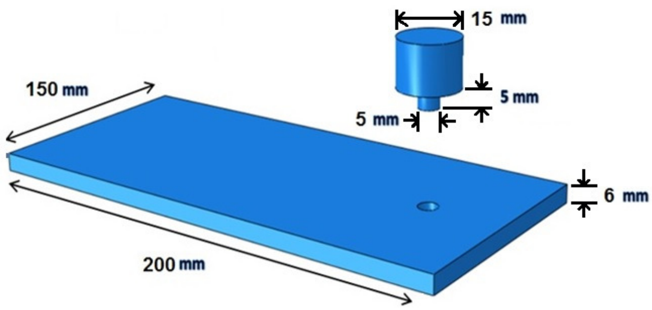

Fig. 4 Modeling generate of FSW by HyperXtrude software

IV. Finite Element Analysis

Two 6061-T6 Al alloy plates, each with a dimension of 150 × 200 × 6 mm are butt welded in the adapted vertical milling machine for FSW when HyperXtrude program is used. In the present thermal analysis, the workpiece is meshed using a brick element called HyperMesh software is used. This element has a 3-dimension thermal conduction capability and can be used for a 3-dimensional, steady-state or transient thermal analysis. Transient finite element analyses are performed considering steady state heat source. The dimension and model are constructed by using HyperMesh and shown in Figs. 3 and 4.

V. Transient Thermal Simulation Model

In the present study, the modeling of friction stir welding is carried out by using HyperXtrude commercial software. This part of software presented the thermal result computed from the model previously. The workpiece has dimensions 150 x 200 x 6 mm; the tool has a shoulder diameter of 15 mm and pin diameter of 5 mm. The rotational speed and welding speed utilized in this comparison are 500, 600, 700 and 800 RPM and 4, 5 and 6 mm/s. On the entire surface of workpiece except the bottom is applied a convective heat transfer of 30 W/m²K whereas for natural convection between workpieces and air.

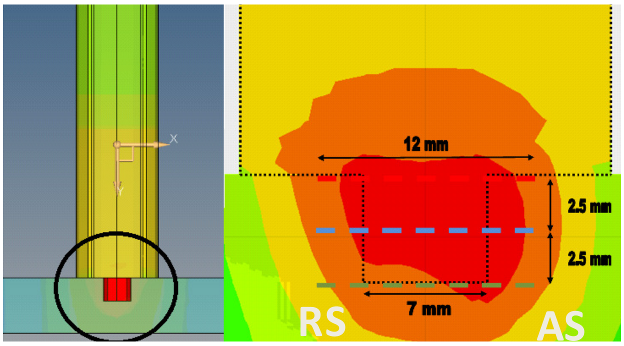

Fig. 5 Temperature divided segment at the pin

A higher convective coefficient of 350 W/m²K is applied as a boundary condition to the bottom surface of the work piece. Transient thermal finite element analyses are performed in order to obtain the temperature distribution in the welded Aluminum plates during the welding operation which is shown in Fig. 5.

TABLE III
Temperature at Pin (°C) (Middle Area)

Rotation Speed (rev/min)	Transverse Speed (mm/s)	Temperature at Pin (°C) (Middle Area)	
		AS	**RS**
500	4	422.4	392.6
	5	413.4	379.3
	6	406.2	368.1
600	4	460.1	428.8
	5	450.4	414.7
	6	442.6	402.6
700	4	493.8	461.2
	5	483.7	446.8
	6	475.5	434.2
800	4	525.0	468.5
	5	514.2	476.3
	6	509.9	503.5

TABLE IV
Temperature at Pin (°C) (Upper Area)

Rotation Speed (rev/min)	Transverse Speed (mm/s)	Temperature at Pin (°C) (Middle Area)	
		AS	**RS**
500	4	406.7	397.2
	5	395.2	386.3
	6	387.4	377.4
600	4	442.5	433.4
	5	432.8	420.1
	6	422.1	411.8
700	4	477.3	465.6
	5	464.8	453.5
	6	455.8	442.9
800	4	504.7	495.4
	5	493.7	481.2
	6	528.4	515.1

TABLE V
Temperature at Pin (°C) (LOWER AREA)

Rotation Speed (rev/min)	Transverse Speed (mm/s)	Temperature at Pin (°C) (Middle Area)	
		AS	**RS**
500	4	403.2	373.5
	5	393.2	358.6
	6	384.1	347.2
600	4	439.6	417.6
	5	428.3	391.4
	6	420.2	379.2
700	4	471.4	438.1
	5	461.6	422.3
	6	451.3	409.8
800	4	503.1	466.9
	5	489.5	450.1
	6	538.9	482.7

The results obtained and divided by 3 main areas of middle area, upper area and lower area (see Tables III-V). The travel speeds are considered in a range of 4-6 mm/s while the tool's rotational speeds are in a range of 500-800 rev/min. As can be seen from the tables, temperature during welding is increased as the rotational speeds increased and also the travel speeds decrease.

Dotted lines show the results obtained in the divided segments of temperature on the pin or near the pin. The upper line (red color) shows the maximum temperature at the top of the pin. The middle line (blue color) shows the maximum temperature at the middle of the pin. The lower line (green color) shows the maximum temperature at the bottom of the pin. From the temperature recorded during the simulation process, the welding temperature distribution at the first start of the process from the welding centerline and welding center surface of the pin could be determine.

As seen from the figures, temperature increases while the rotational speed of the tool increases and travel speed decreases. The maximum temperatures occurred higher at the advancing side which compared to the retreating side of the workpiece.

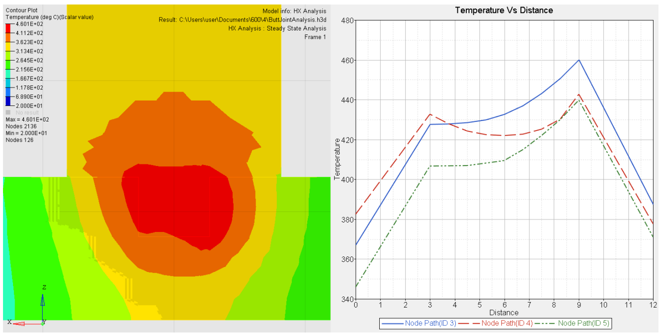

Fig. 6 Temperature distribution obtained by HyperView & HyperXtrude software in welded AA 6061-T6 platesfor rpm =600 rev/min and v= 4 mm/s

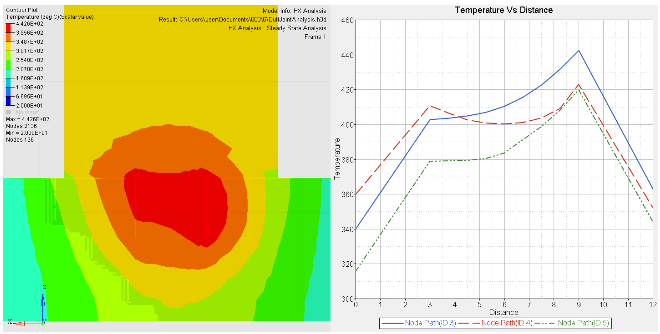

Fig. 7 Temperature distribution obtained by HyperView & HyperXtrude software in welded AA 6061-T6 plates for rpm = 600 rev/min and v= 6 mm/s

This is the effect of the resistance heat which raises the temperature in the stir zone, producing better fluidity and easy plastic deformation. When the simulation process occurs, temperature distribution is asymmetric during the plunge process, which means that the temperature of the advancing side is more intense than the retreating side, resulting in high plastic dissipation on the advancing side.

In this paper, three segments at pin areas are divided in order to describe the temperature changes in the advancing and retreating sides of the process. The segments are utilized to indicate the temperature-distance relationship which is which is shown in Figs. 6 and 7.

When the tool approaches to the material, the temperature goes up quickly. As tool is passing though the welding distance, the temperature begins to fluctuate. Because of the shear friction factor has a negative correlation with the temperature, and the variation of the friction heat affects the temperature. In the welding process, the plasticization material around the tool rotates together with the tool head. The materials from the advancing side flow to the retreating side under the action of the shear friction force, and then it moves back of the retreating side through pin's side. The materials of the retreating side will also undergo rotational flow to the rear of the advancing side, which fills the cavity due to the feeding of the pin.

VI. Conclusion

In the present study, the model of distributed temperatures and its quantities in weld-zones with respect to the process variables such as rotational speed and traveling speed in friction stir process is carried out using the transient finite element analyses facilitated via commercially available software Altair HyperWork. The results obtained show that the increasing tool pin-shoulder rotational speed, at a constant traveling speed, will increase the amount of heat in weld-zones. In contrary, that increasing traveling speed, at constant tool pin-shoulder rotational speeds, will reduce the amount of heat in weld zones. The peak temperature of FSW appeared in rear of the advancing side. The temperature first increased sharply, then experienced a period of fluctuations, and finally the temperature showed a steady decreasing trend. Further study such as observation through experimental works as well as comparing the results obtained via different numerical simulation tools are required to validate the results.

Acknowledgment

The research team wishes to thank to the Ministry of Higher Education Malaysia under the grant number 600-RMI/ERGS 5/3 (82/2012) for the financial support and the Research Management Institute (RMI) of UiTM for the management assistant.

References

[1] G. M. Xie, Z. Y. Ma and L. Geng, "Development of a Fine–Grained Microstructure and Properties of a Nugget Zone in Friction Stir Welded Pure Copper", *Scripta Materiaia*, Vol.57, July 2007.

[2] R.S. Mishra, Z.Y. Ma, "Friction Stir Welding and Processing", Reports: A Review Journal, Sciencedirect, Materials Science and Engineering R 50 (2005), 1-78.

[3] N. T. Kumbhar and K. Bhanumurthy, "Friction Stir Welding of Al 6061 Alloy," *Asian Journal of Experimental Sciences*,Vol.22, no.2, 2008.

[4] J. M. G. de Salazer and M. I. Barrena, "Dissimilar Fusion Welding of AA7020/MMC Reinforced with Al2O3 Particles. Microstructure and Mechanical Properties Materials," *Science and Engineering, A352*, pp.162-168, 2010.

[5] M. A Sutton, B. Yang, A. P. Reynolds and R. Taylor, "Microstructural Studies of Friction Stir Welds in 2024-T3 Aluminum", *Materials Science and Engineering A323 (2002)*, pp.160-166.

[6] M. Cabibo, E. Meccia and E. Evangelista, "TEM Analysis Of Friction Stir Welded Butt Joint of Al-Si-Mg Alloys", *Materials Chemistry and Physics,* Vol.81,no.2-3, August 2003.

[7] M. H. Tolephih, K. M. Mashloosh and W. Zainab, "Comparative Study of The Mechanical Properties of (FS) and MIG Welded Joint in (AA7020-T6) Aluminum Alloys," *Al-Khawarizmi Engineering Journal,* Vol.7, no.2 pp.22-35, 2011.

[8] ASM Handbook, "Properties and Selection: Non-Ferrous Alloys and Special Purposes Materials," *American Society for Metals*, Vol.2, 1992.

[9] J. M. Russelll, "Development and Modelling of Friction Stir Welding," *Thesis, University of Cambridge* (2000)

[10] R. S. Mishra and Z. Y. Ma, "Friction Stir Welding and Processing", *Material Science and Engineering R50 (2005), pp.1-78.*

[11] G. Cam, S. Gucluer, A. Cakan and H. T. Serindag, "Mechanical Properties of Friction Stir Butt Welded Al-5086 H32 Plate", *Journal of Achievements in Materials and Manufacturing Engineering*, Vol.30, no.2, October 2008.

[12] C.M. Chen and R. Kovacevic, "Finite Element Modeling of Friction Stir Welding-Thermal and Thermomechanical Analysis," *International Journal of Machine Tools & Manufacture.* Vol.43, no.13, pp.1319-1326, October 2003.

[13] R. Nandan, T. Debroy and H. K. D. H. Bhadeshia, Recent Advanced in Friction Stir Welding – Process, Weldment Structure and properties," *Progress in Materials Science*, pp.980-1023, August 2008.
[14] S. R. Ren, Z. Y. Ma and L. Q. Chen, "Effect of Welding Parameters on Tensile Properties and Fracture Behavior of Friction Stir Welded Al–Mg–Si Alloy," *Scripta Materialia*, Vol.56, pp.69-72, January, 2007.
[15] P. Colegrove, "3 Dimensional Flow and Thermal Modelling of the Friction Stir Welding Process, *Thesis Master of Engineering Science*, The University of Adelaide, January 2001
[16] Tery Khaled, "An Outsider Looks at Friction Stir Welding," *Ph.D. Thesis*, July, 2005.
[17] R. Nandan, G. G. Roy and T. Debroy, "Numerical Simulation of Three Dimensional Heat Transfer and Plastic Flow During Friction Stir Welding," *Metallurgical and Materials Transactions A: Physical Metallurgy and Materials Science*, Vol. 37, no. 6, pp.1247-1259, 2006.
[18] X. Deng and S. Xu, Solid Mechanics Simulation of Friction Stir Welding Process," *Transaction NAMRI/SME*, Vol.29, pp.631–638, 2001.